

Mitral Annulus Disjunction - An Underdiagnosed Anatomic Morphology: Review of literature

Akhil Mehrotra¹, Faiz Illahi Siddiqui²

¹Chief, Pediatric and Adult Cardiology, Prakash Heart Station, Nirala Nagar, Lucknow, UP, India.

²Cardiac Technician, Prakash Heart Station, Nirala Nagar, Lucknow, UP, India.

Corresponding Author: Dr. Akhil Mehrotra

DOI: <https://doi.org/10.52403/ijshr.20240435>

ABSTRACT

Mitral annular disjunction (MAD) is an easily identifiable entity on transthoracic echocardiography, but is still poorly recognized or ignored. It is often associated with mitral valve prolapse and is itself a risk marker for ventricular arrhythmias and sudden cardiac death.

We present here a case of 54 year Indian male presenting with MVP accompanied by significant mitral annulus disjunction (MAD) in whom a comprehensive transthoracic echocardiography (TTE) and 4Dimensional XStrain speckle tracking imaging was conducted to estimate the MAD distance and importantly, various LV strain parameters were evaluated to discover any early markers of LV aberration by 4Dimensional XStrain speckle tracking echocardiography (4DXStrain STE).

Keywords: Mitral annulus disjunction, MAD, Mitral annulus prolapse, Ventricular arrhythmias in MAD, SCD in MAD, LV strain imaging in MAD.

INTRODUCTION

Mitral annular disjunction (MAD) is a structural abnormality described as the distinct separation between the mitral valve (MV) annulus, the left atrial wall, and the basal portion of the inferolateral left ventricular (LV) myocardium occurring during systole [1]. Mitral annular disjunction (MAD) is an abnormal insertion of the hinge line of the posterior mitral leaflet on the atrial wall: the mitral annulus shows a separation or “disjunction” between the leaflet-atrial wall junction and the crest of the left ventricle myocardium [2] (Figures 1-3).

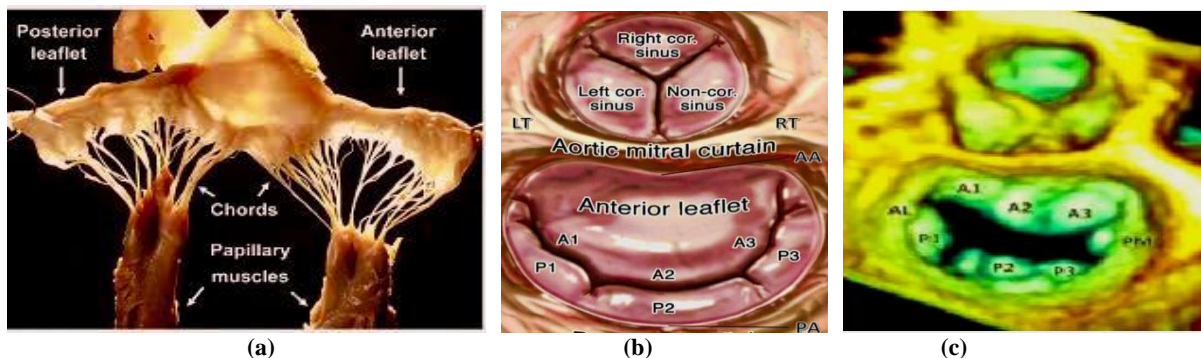


Figure 1: Normal mitral valve apparatus. (a) Anatomical specimen of mitral valve consisting of papillary muscles, tendinous chords, anterior and posterior mitral leaflets; (b) Normal mitral valve anatomy showing anterior and posterior leaflets and annuli. The anterior annulus is separated from the aortic root by the fibrous intertrigonal region, also known as the aortic-mitral curtain, which is surrounded by the right and left fibrous trigones; (c) 3 D TEE image from Surgeon's View of normal mitral valve anatomy as described above. LT = left trigone, RT = right trigone, AA = anterior annulus, PA = posterior annulus, AL = anterolateral commissure, PM = posteromedial commissure.

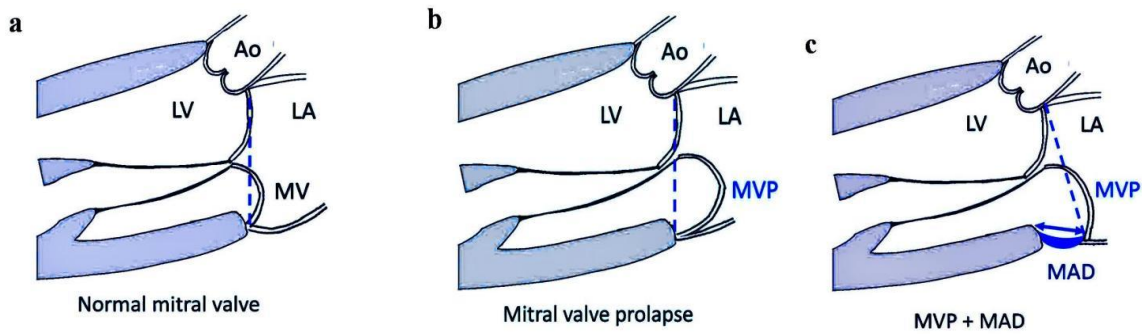


Figure 2: Transthoracic 2D diagrammatic illustration. (a) Normal mitral valve: mitral annular plane is in its normal position (dashed line). (b) Mitral valve prolapse (MVP) without MAD: mitral annulus plane (dashed line) remains in its normal position despite prolapse of the mitral leaflet. (c) MVP with MAD: the mitral annulus is "dislocated" away from the normal left ventricle-left atrial (LV-LA) myocardium junction resulting in MAD (double-arrow), and the mitral annular plane (dashed line) has shifted towards LA. Ao: aorta; LV: left ventricle; LA: left atrium; MV: mitral valve; MVP: mitral valve prolapse; MAD: mitral annulus disjunction.

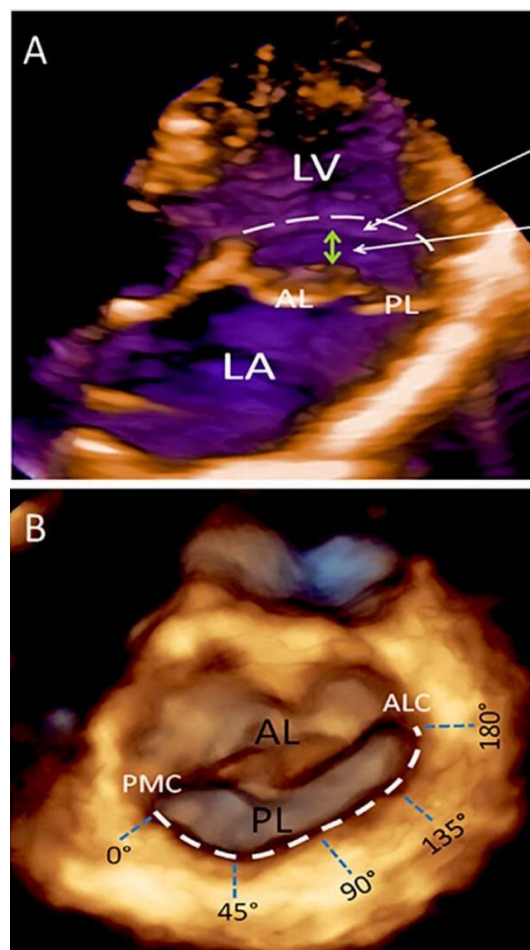


Figure 3: 3D echocardiographic delineation of mitral annulus disjunction. (A) The upper white upper arrow points to the mitral annulus. The lower white arrow depicts the mitral annulus disjunction. (B) Short axis view of the same 3D volume shown in panel A. The mitral valve is seen from an apical view during systole, and a typical atrial excursion of the posterior leaflet appears and indicates the extension of the mitral annulus disjunction. In the present patient, the disjunction involved the complete posterior annulus similar to 180. The disjunction distance was 10 mm, and the disjunction index should be $10 \text{ mm} \hat{=} 180$, that is, $1,800 \text{ mm} \hat{=} \text{degrees}$ (mm $\hat{=} \text{degrees}$). AL, Anterior leaflet; ALC, anterolateral commissure; LA, left atrium; PL, posterior leaflet; PMC, posteromedial commissure.

This anomaly is often observed in patients with myxomatous mitral valve prolapse [2].

The anatomical substrate of MAD remains unclear for the following reasons:

1. Most studies are focused on the association between MAD and arrhythmias, rather than an pathomorphological aspects of MAD
2. The complex anatomic architecture of the posterior mitral annulus is often described as the posterior segment of a fibrous ring.

Currently, it is unclear if MAD is a degenerative, congenital, or an acquired structural abnormality. Researchers suggest that this condition is the result of increased stretching and mechanical stress on the MV annulus, which causes an increase in tissue formation that develops into prolapsing segments [3]. This condition has been strongly associated with myxomatous MV and MV prolapse (MVP). MAD has been associated with long-term incidence of ventricular arrhythmias and sudden cardiac death [4]. The proper detection of MAD is important given our increased understanding of an association between MAD and arrhythmic events. In this case presentation we describe the complementary value of

transthoracic echocardiography (TTE) and 4Dimensional XStrain speckle tracking echocardiography (STE) in detecting and classifying MAD and additionally unmask any early features of LV dysfunction by STE.

Definition of mitral annulus disjunction, mitral valve prolapse and billowing of mitral valve

On cardiac magnetic resonance (CMR) MAD is defined as present when it measures 1 mm or more [5]. In CMR where disjunction was observed, it was measured from the top edge of the ventricular wall to the hinge of the leaflet from the left atrial wall, parallel to disjunction at end-systole (Figure 4). The end-systolic phase was selected by determining the phase in which the intracavity ventricular blood pool was at its smallest. The 3-chamber view was assessed for the presence of either mitral valve prolapse (MVP) or Mitral valve billowing (MVB) of either leaflet of the mitral valve (Figure 4).

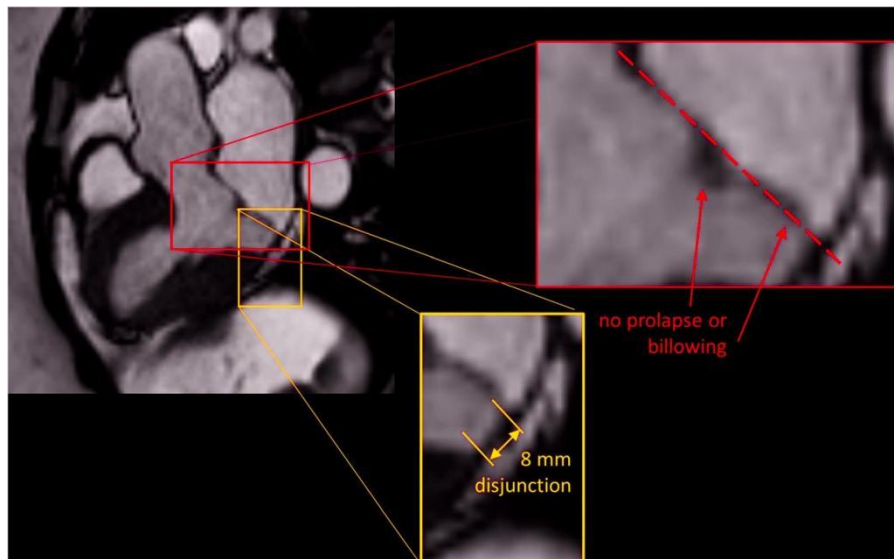


Figure 4: CMR in a Patient With Inferolateral Disjunction Without Mitral Valve Prolapse or Billowing. CMR 3-chamber long-axis view (upper left) with enlarged details displaying measurement of inferolateral disjunction (yellow frame) and absence of mitral valve prolapse or leaflet billowing (red frame) as assessed by drawing a line in the virtual annular plane (red interrupted line).

On TTE MVP was classified as systolic displacement of any part of the leaflet by 2 mm or more from the annular plane into the

left atrium in 3-chamber view as recommended by the American Society of Echocardiography [6] (Figure 5).

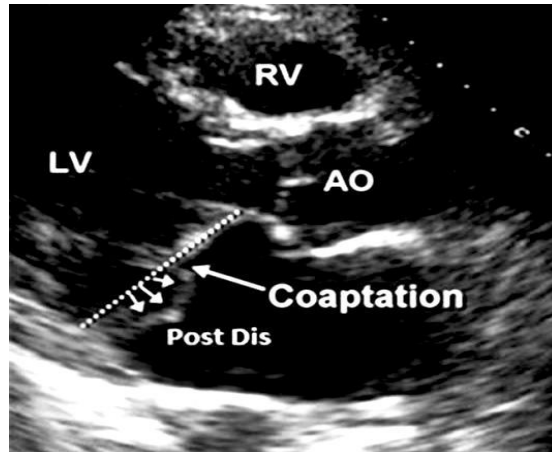


Figure 5: 2Dimensional transthoracic echocardiographic definition of mitral valve prolapse. Two-dimensional transthoracic echocardiogram in the parasternal long-axis orientation demonstrating posterior mitral valve prolapse (MVP). MVP shows diagnostic (>2 mm) superior leaflet displacement relative to the mitral annulus (dotted line) into the left atrium. AO indicates aorta; LV, left ventricle; Post Dis, posterior displacement; and RV, right ventricle.

MVB was defined as systolic protrusion of the leaflet of <2 mm above the junctional

plane with the coaptation point at or below the plane at end-systole (Figure 6).

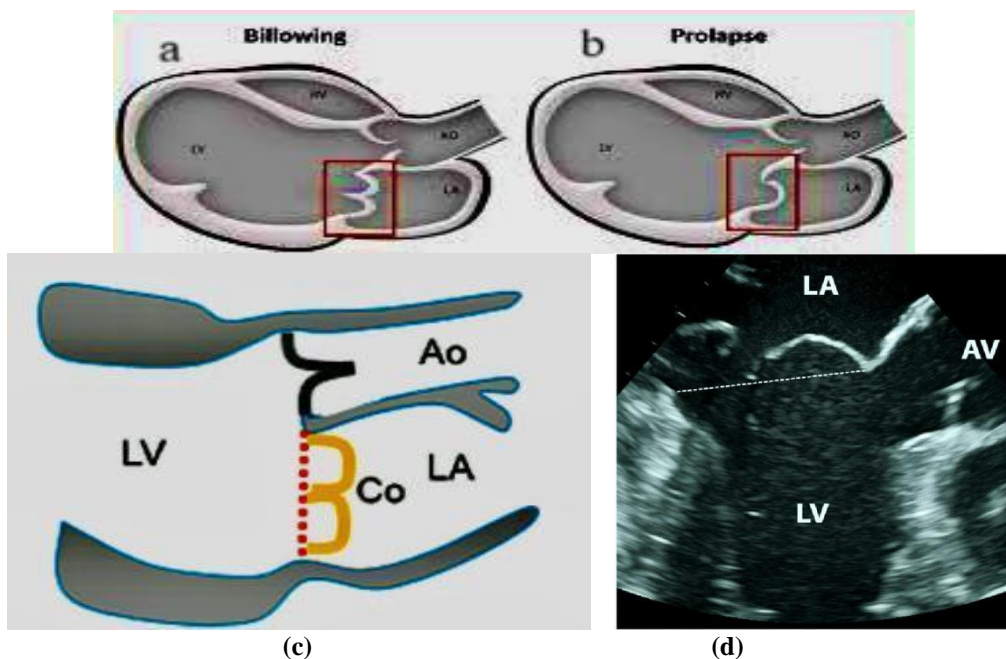


Figure 6: Mitral Valve Billowing in end systole - schematic portrayal and Transesophageal echocardiogram of mitral valve billowing. (a) Billowing: leaflet body displaced into LA, leaflet tips stay at annular level or above into LV; (b) Prolapse: leaflet tips displaced into LA from mitral annular plane; (c) Mitral valve billowing in long axis view - red dotted line is a reference point. billowing with free edge of both mitral leaflets protrudes into the LA (yellow color); (d) Transesophageal echocardiogram of mitral valve billowing-the free edge of both leaflets overrides the plane of displaced mitral valve annulus (dotted line) in systole.

MAD - Left ventricular strain imaging by speckle tracking echocardiography

Despite that MAD could be present in healthy hearts, some authors revealed its connection with the arrhythmic MVP phenotype [4, 7, 8]. MAD leads to the

excessive mobility of the leaflets, accounting for a mechanical stretch of the inferobasal wall and papillary muscles, eventually leading to myocardial damage and fibrosis [9] as a possible substrate for ventricular arrhythmias (VA's).

Speckle tracking echocardiography (STE) allows a precise measure of myocardial segmental systolic deformation. STE has been shown to reveal subclinical abnormal deformation [10] and it may offer new insights in the understanding of mitral valve and myocardial interactions in patients of MAD accompanied by MVP [10].

MAD is an increasingly recognized entity associated with MVP, ventricular arrhythmias and death. Wang et al [11] investigated the utility of myocardial deformation analysis in MAD. They found that patients with MAD and MVP had lower basal longitudinal strain by TTE than those with MVP without MAD. Correspondingly, those with MAD and MVP had lower magnitude of circumferential and radial strain analyzed by CMR, in basal inferolateral and basal segments compared to those with MVP without MAD and controls.

CASE REPORT

A 54 year adult male presented to our cardiology OPD with the complaints of

atypical chest pain and occasional palpitations. The palpitations were for only few seconds. Even though the patient was hypertensive, he was currently, controlled on appropriate medications. The patient denied any history of other cardiovascular risk factors (smoking, tobacco chewing, diabetes, dyslipidemia), thyroid disorders and any episode of syncope.

On clinical examination, the patient was healthy looking and normally built. The patient's weight was 71 kg, height was 158 cm, pulse rate was 86/min, blood pressure was 130/80 mmHg on anti-hypertensive medications, respiratory rate was 16/min and SPO2 was 98% at room air. All the peripheral pulses were normally palpable without any radio-femoral delay.

On cardiovascular examination, there was presence of mid systolic click followed grade 2/4 mid systolic murmur over the LV apex, best heard in the left lateral decubitus position. LV S3 gallop was absent. Rest of the systemic examination was normal.

Xray chest (PA) view and resting ECG were normal (Figure 7).

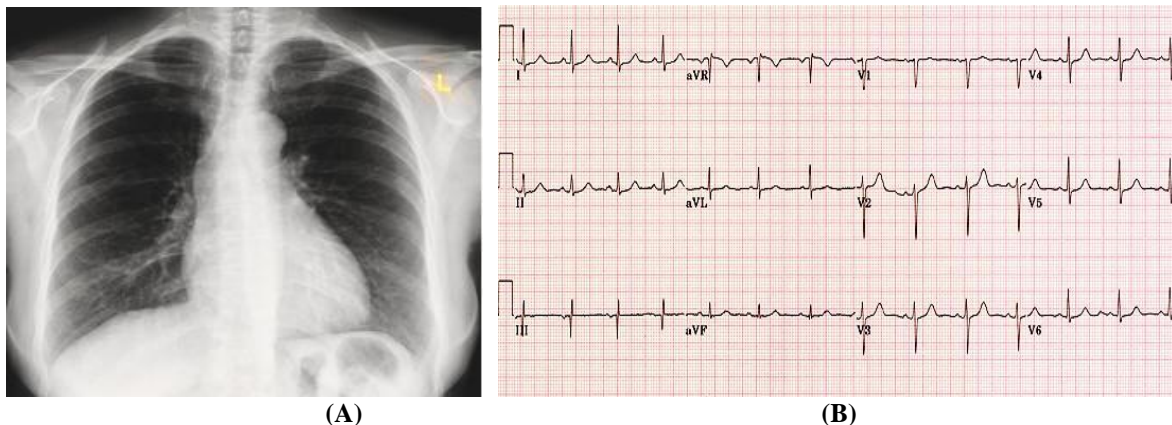


Figure 7: X-ray chest (PA) view normal; (B) Resting ECG normal

Moreover, the pathological investigations for estimation of diabetes, dyslipidemia and thyroid profile were normal. The standard Bruce protocol treadmill stress test and 48 hour holter monitoring to detect the presence of any arrhythmia, were within normal limits.

Transthoracic Echocardiography

All echocardiography evaluations were performed by the author, using My Lab X7 4D XStrain echocardiography machine, Esaote, Italy. The images were acquired using an adult probe equipped with harmonic variable frequency electronic single crystal array transducer while the subject was lying in supine and left lateral decubitus positions.

Conventional M-mode, two-dimensional and pulse wave Doppler (PWD) and continuous wave doppler (CWD) echocardiography was performed in the classical subcostal, parasternal long axis (LX), parasternal short axis (SX), 4-Chamber (4CH), 5-Chamber (5CH) and suprasternal views (Figures 8-15).

M-mode Echocardiography

M-mode echocardiography of left ventricle was performed and the estimated measurements are outlined (Table 1, Figure 8).

Table 1: Calculations of M-mode echocardiography

Measurements	LV
IVS d	7.7 mm
LVID d	58.5 mm
LVPW d	6.5 mm
IVS s	13.4 mm
LVID s	34.8 mm
LVPW s	14.2 mm
EF	70 %
% LVFS	41 %
LVEDV	170.1 ml
LVESV	50.2 ml
SV	119.9 ml
LV Mass	153 g

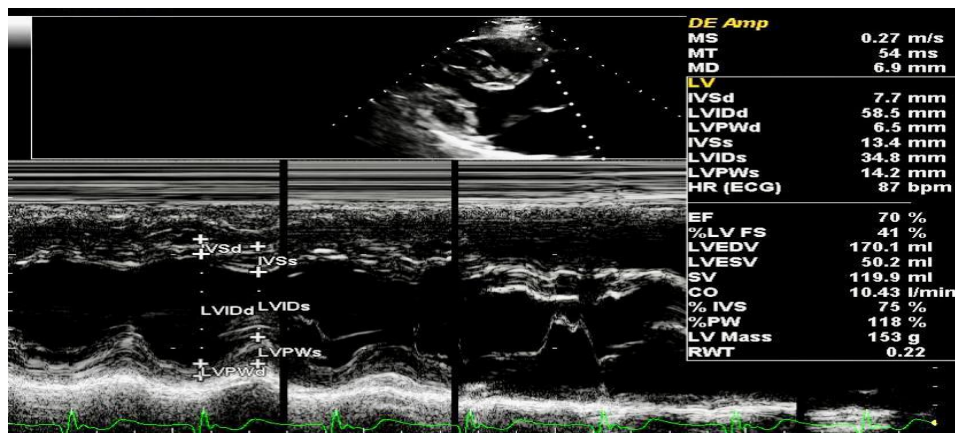


Figure 8: M-mode measurements of left ventricle

Summary of M-mode echocardiography

The LV was dilated with an LV internal dimension in diastole and LVEDV being 58.5 mm and 170.1 ml, respectively. The LVEF was normal -70%.

2Dimensional color echocardiography

Transthoracic color echocardiography exhibited multiple features as outlined below:

- Levocardia
- Situs solitus
- A-V concordance
- V-A concordance
- Concordant D-bulboventricular loop
- Normally related great arteries (NRGA)
- Left aortic arch

- Normal pulmonary and systolic venous drainage

In the LX view, there was conspicuous presence of mitral valve prolapse of AML and PML. The superior displacement of AML and PML was 3.7 mm and 4.2 mm, respectively (Figure 9). However, the MV leaflets were thickened and the mitral annulus was dilated (D=35.5 mm). A significant mitral regurgitation was demonstrated (Figure 10). MR jet area was 3.69 sqcm, visualized as an eccentrically directed posterior jet. Mitral annulus disjunction (MAD) was delineated (Figure 11), and the MAD distance was 9.3 mm.

4Dimensional volumetric data

Table 2 depicts the volumetric data acquired by 4Dimensional XStrain echocardiography

Table 2: 4Dimensional volumetric data

Parameters	Values
LVEDV	80.81 ml
LVESV	29.96 ml

EF	62.93 %
CO	4438.98 ml/min
Sph i d	0.39
Sph i s	0.25
EDV, end diastolic volume; ESV, end systolic volume; EF, ejection fraction; CO, cardiac output; Sph i d, sphericity index diastole; Sph i s, sphericity index systole	

Speckle tracking echocardiography by 4Dimensional XStrain technique. The Comprehensive speckle tracking values obtained of various LV strain echocardiography (STE) was accomplished parameters are enumerated (Table 3):

Table 3: 4Dimensional XStrain echocardiography - estimated values of LV strain parameters in our index patient

LV strain Parameters	Strain (%)	Strain rate (1/s)
Global longitudinal strain (GLS)		
AP 2C	-19.28	1.97
AP LAX	-17.76	1.91
AP 4C	-16.41	1.85
Global strain	-17.81	-
Global circumferential strain (GCS)		
at MV level	-15.04	1.04
at pap mus level	-10.77	1.51
Global radial strain (GRS)		
at MV level	28.78	1.54
at pap mus level	21.94	2.71
AP, apical; 2C, two chamber; LAX, long axis; 4C, four chamber; MV, mitral valve; pap mus, papillary muscle.		

Table 4: 4Dimensional XStrain echocardiography estimation of LV segmental endocardial longitudinal strain

Bull's eye analysis		
Endo long strain (Peak)		
Bas Ant	-21.95	%
BasAntSep	-5.69	%
Bas Sep	-12.63	%
Bas Inf	-20.14	%
Bas Post	-41.04	%
Bas lat	-34.88	%
Mid Ant	-27.26	%
MidAntSep	-14.71	%
Mid Sep	-11.03	%
Mid Inf	-15.21	%
Mid Post	-8.95	%
Mid Lat	-15.99	%
Apic Ant	-18.95	%
Apic Sep	-25.34	%
Apic Inf	-18.26	%
Apic lat	-15.93	%
Apex	-16.18	%
Global Strain (A2C)	-19.28	%
Global Strain (ALAX)	-17.76	%
Global Strain (A4C)	-16.41	%
Global Strain	-17.81	%

Red squares depict significant reduction in strain values in multiple segments of LV

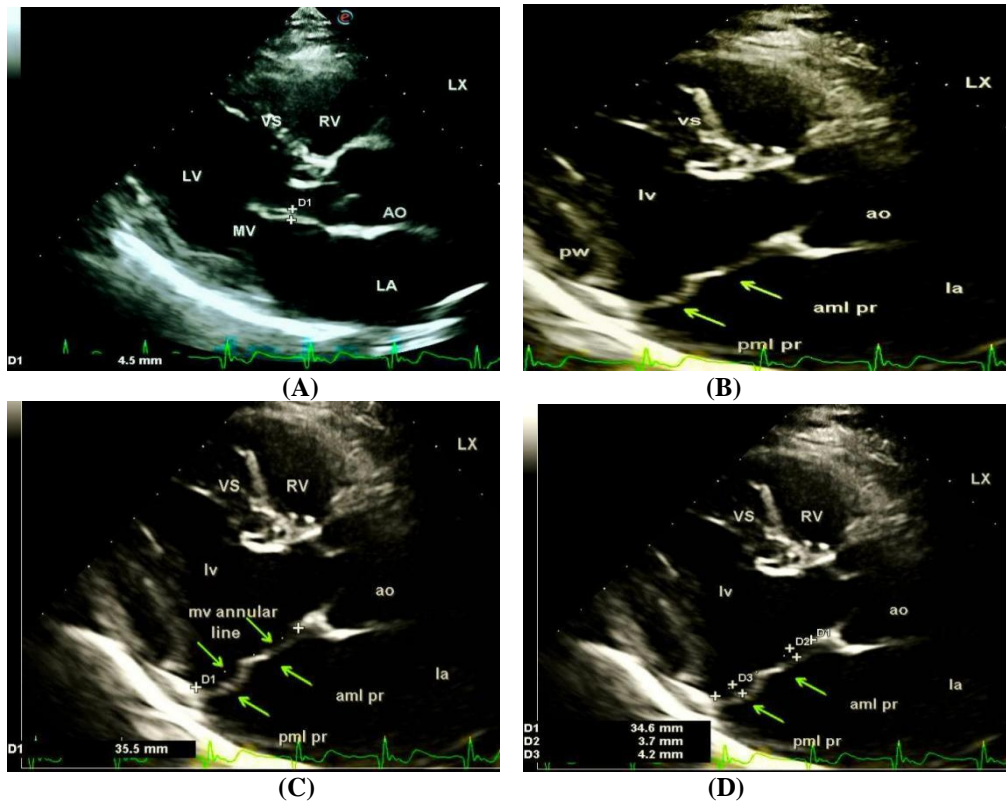


Figure 9: 2Dimensional transthoracic Echocardiography of mitral valve prolapse. (A) LX view shows thickened mv leaflets; (B) LX depicting superior displacement of AML and PML; (C) LX shows dilatation of mitral valve annulus (D=35.5 mm); (D) LX illustrates the superior displacement of AML and PML from the mitral annular plane of 3.7 mm and 4.2 mm respectively



Figure 10: Mitral regurgitation. LX reveals the presence of moderate mitral regurgitation. The area of the jet was 3.69 sqcm.

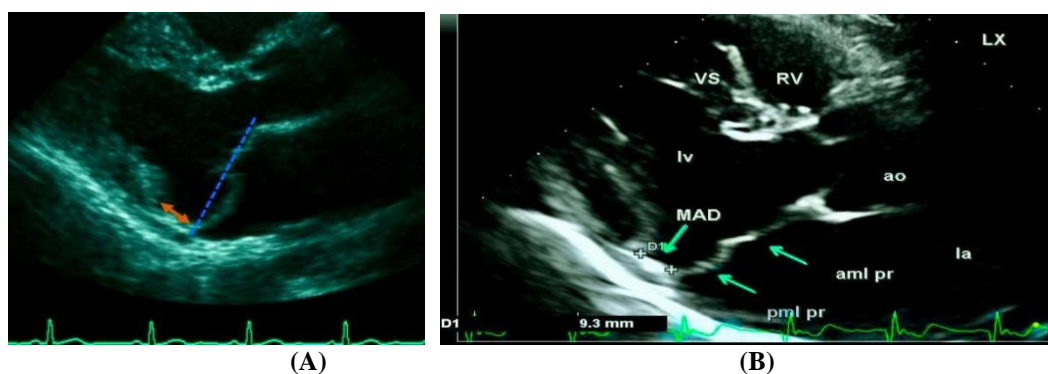


Figure 11: Mitral annulus disjunction (MAD). (A) 2D echocardiographic illustration of MAD in LX view; (B) MAD in our patient was 9.3 mm

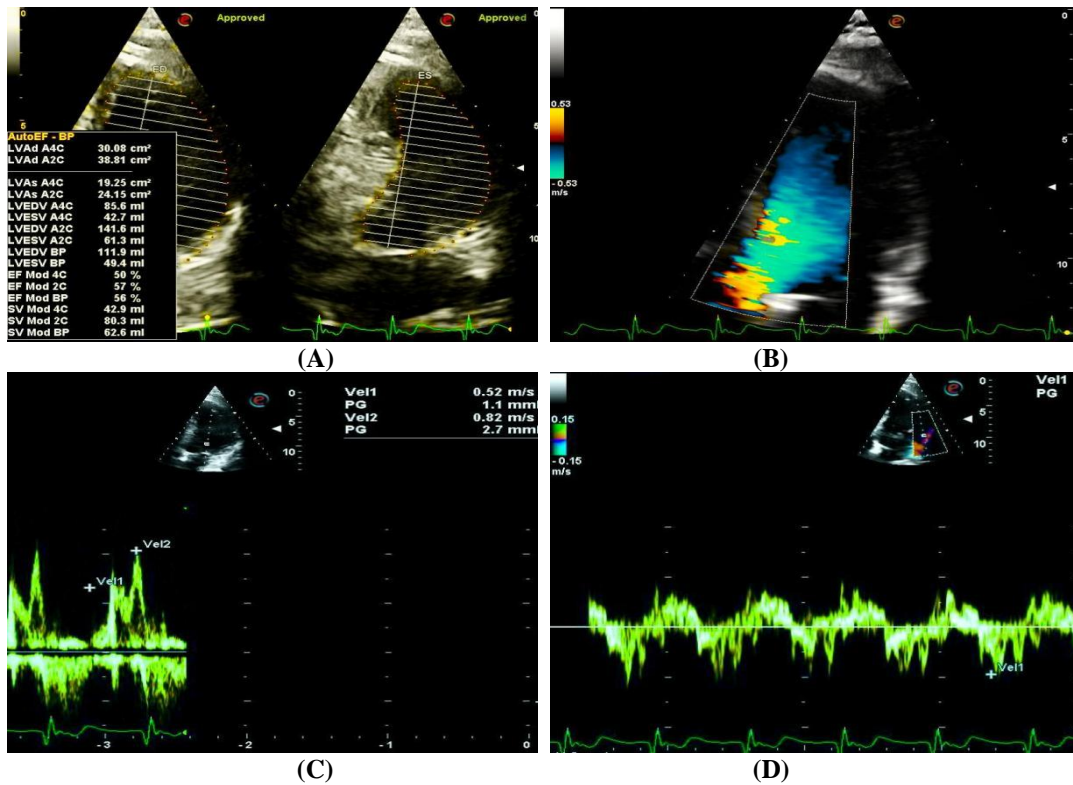


Figure 12: Illustration of LVEF by biplane Simpson's method, absence of LVOT obstruction, pulse wave doppler pattern of mitral velocities and lateral wall LV tissue doppler imaging in our patient. (A) Biplane Simpson's method LVEF was 56 %; (B) Absence of LVOT obstruction in 5C view; (C) Mitral valve velocity reveals LV diastolic relaxation dysfunction grade 1; (D) TDI of lateral wall of LV.

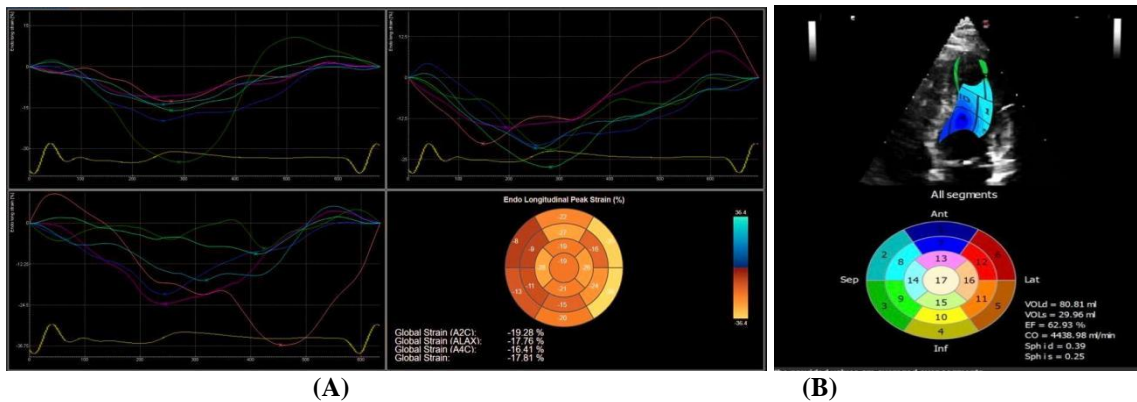
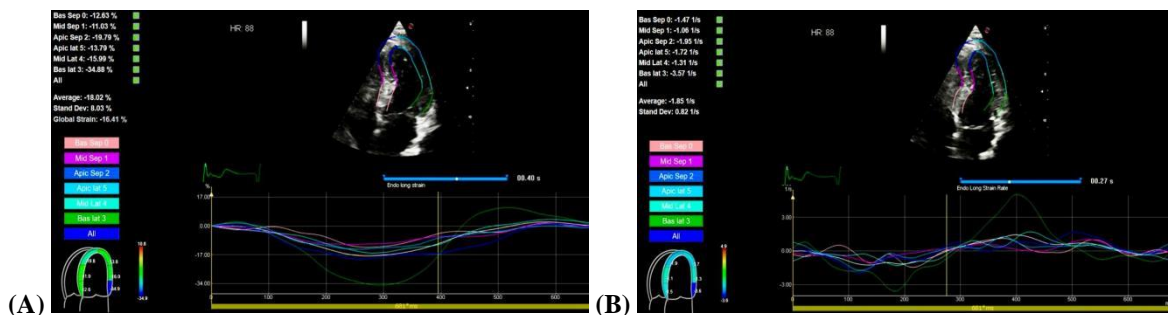


Figure 13: 4Dimensional XStrain speckle tracking echocardiography. (A) Bull's eye plot and graphs of peak endocardial longitudinal strain; (B) 4Dimensional volumetric data derived from XStrain 4D echocardiography.



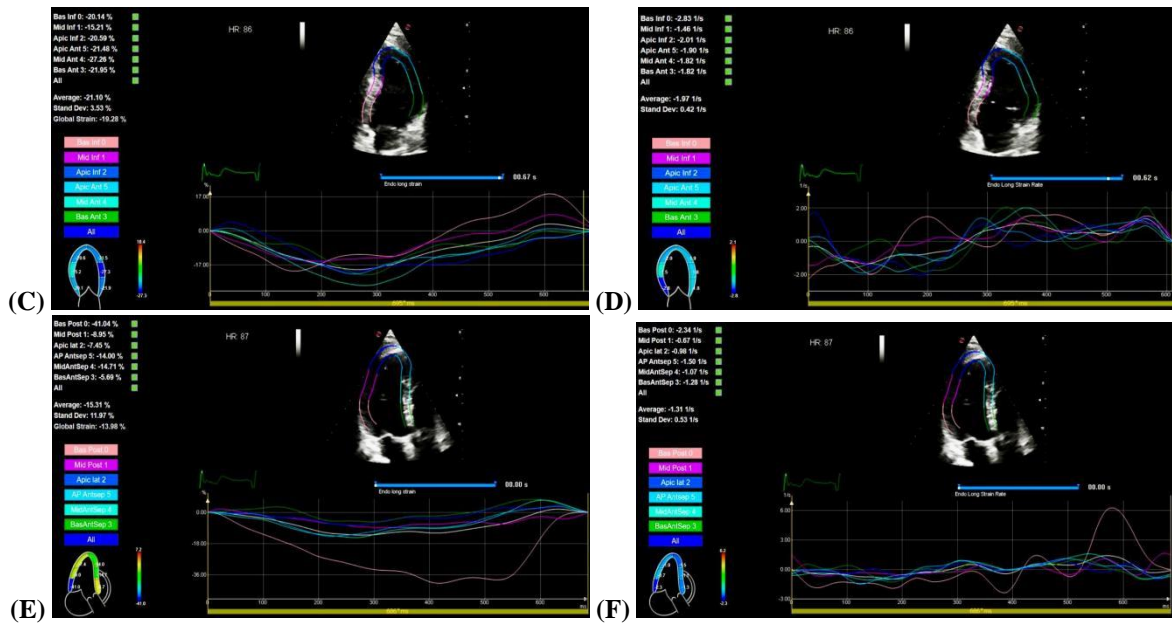
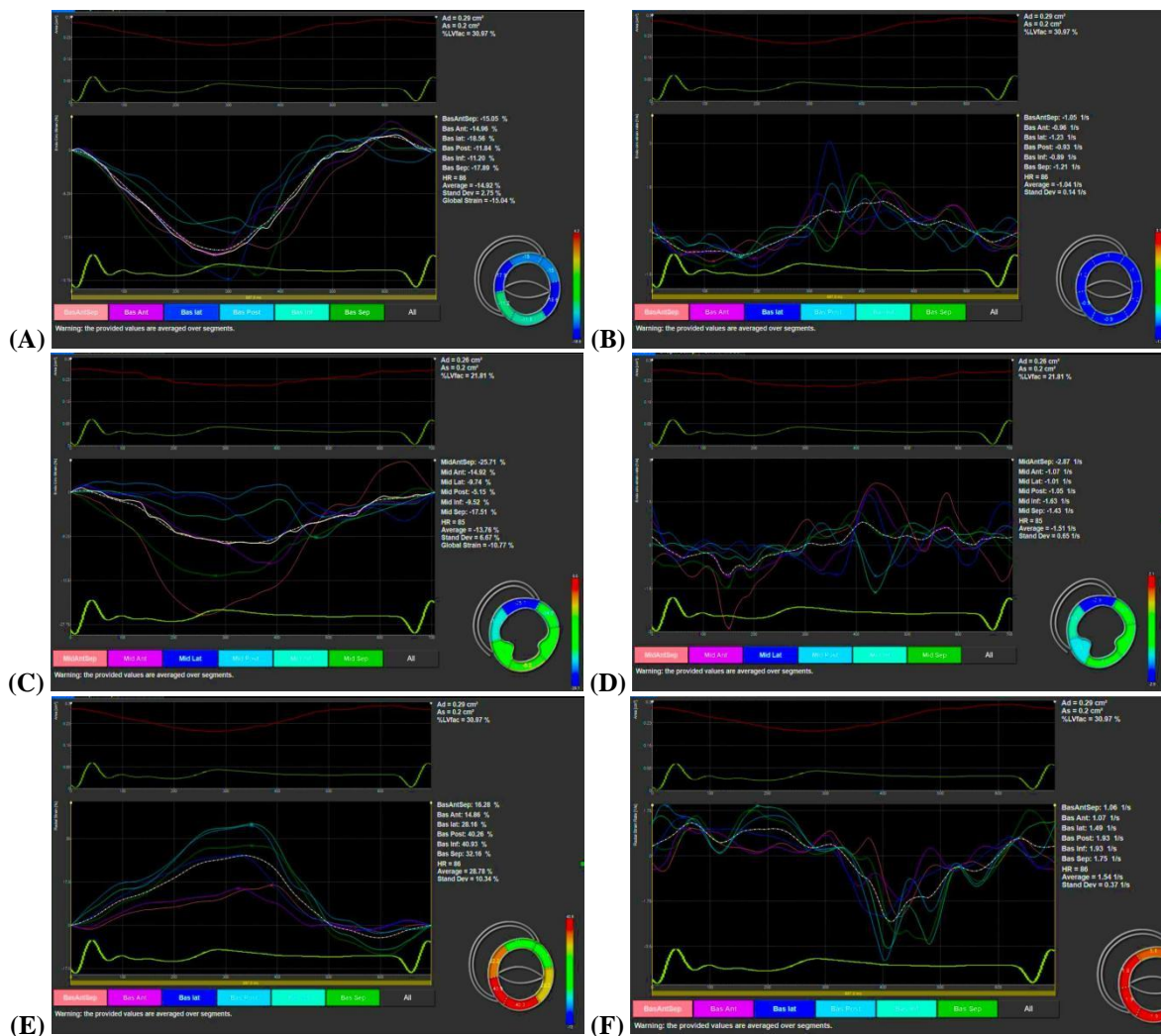


Figure 14: 4Dimensional XStrain Echocardiography. Global longitudinal strain and strain rate of AP4C, AP2C and APLAX views. (A) 4C global longitudinal strain; (B) 4C global longitudinal strain rate; (C) 2C global longitudinal strain; (D) 2C global longitudinal strain rate; (E) LAX, global longitudinal strain; (F) LAX, global longitudinal strain rate; AP, apical; 4C, four chamber; 2C, two chamber; LAX, long axis



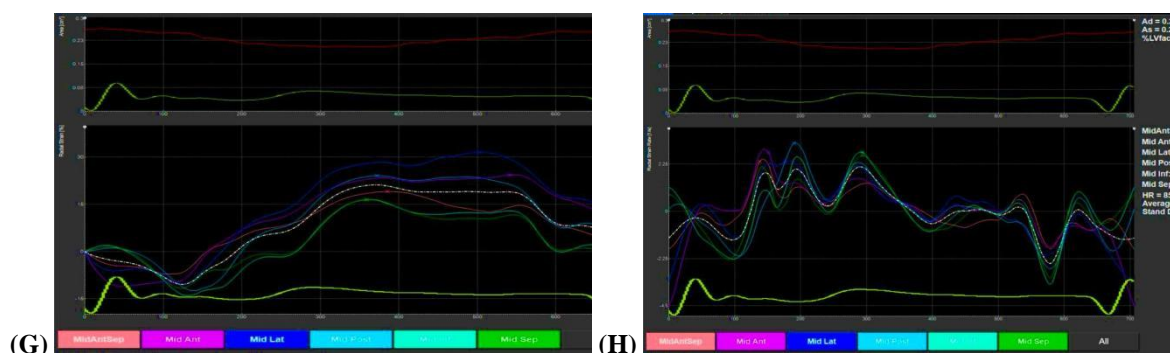


Figure 15: 4Dimensional XStrain Echocardiography. (A) Global circumferential strain, at MV level; (B) Global circumferential strain rate, at MV level; (C) Global circumferential strain, at papillary muscle level; (D) Global circumferential strain rate, at papillary muscle level; (E) Global radial strain, at MV level; (F) Global radial strain rate, at MV level; (G) Global radial strain, at papillary muscle level; (H) Global radial strain rate, at papillary muscle level

Summary of 2Dimensional transthoracic and 4Dimensional XStrain speckle tracking echocardiography

Our index patient, a known hypertensive controlled on anti-hypertensive medications, presented to us with history of atypical chest pain and occasional palpitations. In the backdrop of normal treadmill stress test, holter and various pathological investigation conducted, we performed a comprehensive TTE and 4D XStrain STE with the aim to estimate the mitral annulus disjunction, and moreover, to demonstrate any early features of LV systolic dysfunction by detecting aberrancy in various LV strain parameters acquired by 4D XStrain STE.

In the standard 2Dimensional TTE we demonstrated primary prolapse of AML and PML, dilatation of mitral valve annulus, moderate grade mitral regurgitation, dilation of LV and MAD distance of 9.3 mm.

On 4D XStrain STE, we illustrated: GLS value of -17.81 %, GCS values at MV and pap mus level of -15.04 % and -10.77 % respectively and GRS values at MV and pap mus level of 28.78 % and 21.94 % respectively. The values of GLS and GCS were lesser than the values of normal 4D STE and 4D XStrain STE, in healthy adults [12, 13]. Furthermore, on segmental LV endocardial longitudinal strain analysis, we delineated significant reduction in strain values in multiple segments (Table 4).

DISCUSSION

Epidemiology

Mitral annulus disjunction has been reported in 42-90% of patients with myxomatous mitral valve disease and mitral prolapse [1]. The prevalence of MVP is variable. The worldwide prevalence of MVP is between 0.4% and 35% whereas Indian prevalence by echocardiography studies is between 2.7% and 16% [14, 15]. This wide prevalence could be due to the variety of populations studied, both hospital-based and healthy volunteers with a minority still being unrecognized since most are usually asymptomatic. There are very few autopsy studies on MVP with a reported incidence of about 4%-5% at autopsy [16, 17].

MVP is more common in females as compared to males [14]. Myxomatous degeneration is the most common cause of MVP in which there is excessive accumulation of glycosaminoglycan material within leaflets and cusps. Other less common causes include dysfunctional papillary muscles, ruptured chordae tendineae or papillary muscles [18, 19].

Mitral annulus disjunction

Mitral annulus disjunction is an anatomic abnormality involving the confluence of the left atrium, mitral valve annulus, and the base of the left ventricle (Figure 16). It is classically associated with the spectrum of myxomatous disease of the mitral valve and MVP [18, 19].

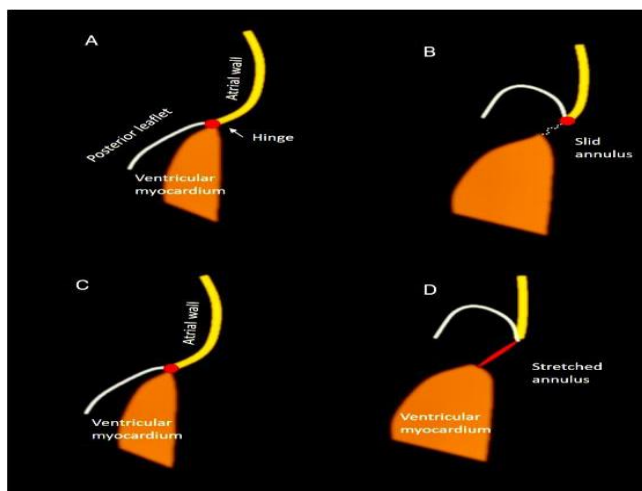


Figure 16: (A, B) First hypothesis on MAD morphology. Although the posterior hinge line is somehow detached by the myocardium, it maintains its own "normal" position. In systole, as the posterior myocardium contracts, the hinge line slides backward, and MAD becomes visible. Which structure/tissue fills the gap between the hinge line and the crest of ventricular myocardium is unclear. (C, D) Second hypothesis: in systole the hinge line is stretched.

History and etymology

The term 'mitral annular disjunction was first used by Bharati et al. in 1981 and later defined by Hutchins et al. in 1986 [20, 21].

Associations

Mitral annular disjunction has been associated with the following clinical conditions [1-4]:

- mitral valve prolapse (MVP)
 - particularly bileaflet prolapse [22]
- myxomatous degeneration of mitral leaflets
- sudden cardiac death
 - ventricular ectopy and dysrhythmias

Classification

I. A suggested classification for subgrouping MAD by measured degree of disjunction was proposed in 2013 by Konda et al. [23]:

- type I: excessive annular mobility with an absence of a visualized separation between annulus and basal left ventricular myocardium
- type II: annulus-ventricular separation (i.e. disjunction) of less than 5 mm
- type III: disjunction greater than 5 mm

II. Another similar classification was recommended by Konda et al, 2020 [24].

The study analyzed TTE results of 185 patients with severe mitral regurgitation (MR) due to MVP. In this analysis, the researchers classified patients into four subtypes based on valve annulus mobility:

- Type 0 - No MAD
 - Type I - Hypermobile basal left ventricular segment without MAD
 - Type II - MAD < 5 mm
 - Type III - MAD > 5 mm.
- Interestingly, the percentage of patients classified as:
- Type I were 65.5 %
 - Type II were 25.4 %
 - Type 0 were 7.6 %
 - Type III were 0.5 %

Increased severity of MAD has been found to correlate with:

- degree of mitral regurgitation [25]
- number of valve segments with flail or prolapse
- increasing burden of ventricular dysrhythmias

Risk predictors for ventricular arrhythmia in patients with MAD is outlined in Table 5.

Table 5: Risk predictors for ventricular arrhythmias in patients with MAD [26]

Physical Exam
Mid-systolic click
Electrocardiographic
Biphasic/inverted T waves, especially inferolateral leads
ST-segment depressions
QT dispersion/prolongation
PVCs with right bundle branch block pattern, especially from LVOT or papillary muscles
Morphologic/Imaging
MAD distance, especially > 8.5 mm
Bileaflet MVP
Mitral valve leaflet thickness of ≥ 5 mm on M-mode
Larger LA and LV end-systolic diameter
Annular dilation
Lower global longitudinal strain
Paradoxical systolic increase in mitral annular diameter
Increased tissue Doppler velocity of lateral mitral annulus; Pickelhaube sign
Higher mechanical dispersion
Lower EF
Papillary muscle fibrosis
LV fibrosis, especially inferobasal wall
Increased extracellular volume in basal segments on CMR
Blomarkers
Elevated sST2

EF = ejection fraction; LA = left atrium; LV = left ventricle; LVOT = left ventricular outflow tract; MAD = mitral annular disjunction; MVP = mitral valve prolapse, PVC = premature ventricular complex; SCD = sudden cardiac death; sST2 = soluble suppression of tumorigenicity 2.

Risk stratification of MAD patients

The following protocol is typically used for risk stratification of MAD patients [27]. All patients with echocardiographically detected MAD accompanied by signs of mechanical stretch (high longitudinal strain values in basal inferolateral wall/"Pickelhaube" sign, inverted T waves in inferior leads) and frequent ventricular arrhythmias arising from posterior papillary muscle/outflow tract (12-lead ECG Holter monitoring and treadmill test), should be further tested with CMR to detect myocardial or papillary muscle fibrosis. In cases of symptomatic VTs or LGE/diffuse fibrosis, EPS should be performed to further map the site of ectopic activity and to reveal possible multifocality, along with programmed ventricular stimulation. Patients with "positive" EPS

should be referred for implantable cardioverter defibrillator (ICD) implantation. In accordance with the recently announced risk stratification algorithm of European Heart Rhythm Association, asymptomatic patients without complex ventricular may be further monitored with an implantable loop recorder (ILR), while MVP patients with no documented arrhythmias, but other malignant phenotypic characteristics (as previously described) may be candidates for ILR, or frequent monitoring [27].

Echocardiography

TTE is considered is usually the first-line imaging modality for the evaluation of mitral valvular disorders [1] (Figure 17).

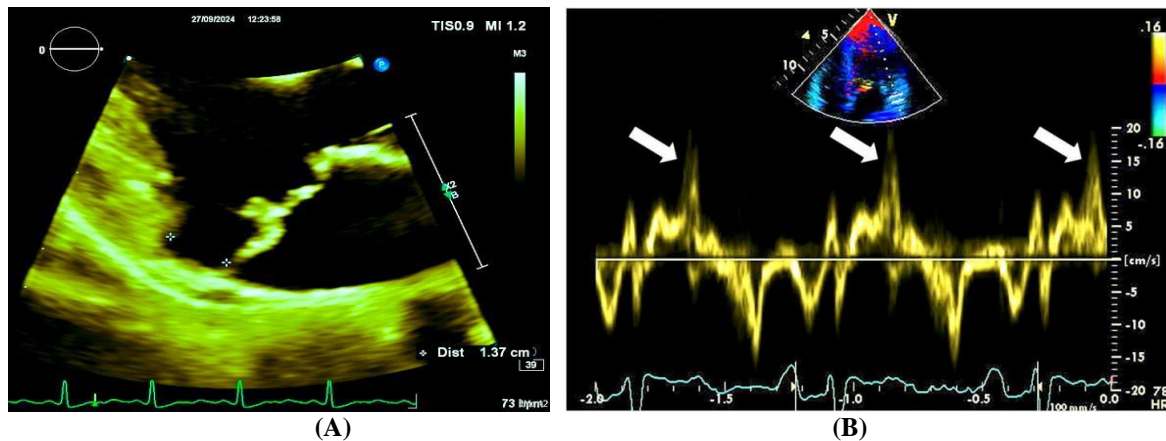


Figure 17: (A) TTE demonstration of measurement of MAD in systole; (B) Pickelhaube sign - reflects increased velocity at the lateral mitral annulus in mid-systole to late-systole. The velocity spike is denoted by a white arrow. Pickelhaube sign maybe indicative of high risk in MAD.

Toh et al [28], in a recent review of 98 subjects with structurally normal hearts, reported that 96% had MAD. No minimum distance was used to define MAD positivity, and the median MAD distance was just 3.0 mm with a range of 1.5 to 7 mm. This is much lower than the average MAD distance noted in many studies involving patients with MVP. Mantegazza et al [29] reported an average MAD distance of 6.6 ± 2.2 mm in surgical patients with MVP and MAD on TTE. Similarly, Essayagh et al [30] found an average MAD distance of 8 ± 4 mm in patients with MVP who were diagnosed with MAD by CMR. Konda et al [23] set a minimum MAD distance of 2 mm by TTE to be considered to have MAD.

Thus, the majority of people, including those with structurally normal hearts, may have some minimal degree of MAD that is more readily identified as the spatial resolution of cardiac imaging improves. The question is then raised of what distance of disjunction represents clinically significant MAD. An early study found that a MAD distance of >8.5 mm by TTE was associated with higher likelihood of NSVT [31]. Perazzolo Marra et al [32] found that MVP patients with LV fibrosis on CMR had a median MAD distance of 4.8 mm, whereas the median MAD distance was only 1.8 mm in MVP patients without LV fibrosis. A more recent study of Lee et al [33] using CMR found an association between the 3-dimensional extent of MAD and mitral

regurgitant orifice area. It may be that "pathological" MAD has a more extensive circumferential distribution as well as a greater distance when compared with the MAD seen in normal variants. More research is needed to clarify how the extent of MAD-both maximum distance and circumferential extent-relates to clinical outcomes, to establish a threshold for clinically significant MAD.

In our patient, MAD distance was 9.3, on TTE in the long axis view.

Left ventricular strain imaging in MAD

Few studies have investigated the utility of myocardial deformation analysis in MAD [11]. Forty-two patients with MVP (21 with MAD, 21 without MAD) and 21 controls were studied. Global, basal and basal inferolateral segmental strains were measured and compared using velocity-vector imaging TTE and feature-tracking CMR [11].

Another study aimed to evaluate left ventricular (LV) function using speckle tracking echocardiography in MVP patients with MAD [34]. Transthoracic echocardiography and cardiac magnetic resonance imaging were performed to assess LV function and MAD presence. Late gadolinium enhancement frequency was significantly higher in MAD patients with MVP. MAD patients with MVP had significantly impaired global longitudinal strain, basal longitudinal strain, mid-

ventricular longitudinal strain and LA strain when compared to MVP patients without MAD, despite similar LV ejection fraction. All these values of MVP patients were also significantly lower than the control group. The mean MAD distance was 7.8 ± 3.2 mm in MAD patients with MVP. This study demonstrated a significant decrease in longitudinal strain in MVP patients with MAD, indicating myocardial dysfunction. These findings suggest that MAD may contribute to LV dysfunction and highlight

the importance of early detection in younger patients.

In our patient, there was significant alteration in values of GLS and GCS. Moreover, the segmental endocardial longitudinal strain displayed marked reduction in strain values in multiple segments of LV. Normal values of 2Dimensional and 4Dimensional LV strain in healthy subjects is shown in Table 6 and 4Dimensional XStrain STE analysis in healthy adults is outlined in Table 7.

Table 6: 2Dimensional and 4Dimensional LV strain values in healthy subjects [12].

LV parameters	median %	1st - 3rd quartiles
2D Longitudinal strain	-21	-20 to -23
2D Circumferential strain	-22	-20 to -24
2D Radial strain	46	39 to 54
4D Longitudinal strain	-19	-17 to -21
4D Circumferential strain	-18	-17 to -20
4D Radial strain	52	47 to 59

Table 7: 4Dimensional XStrain LV deformation parameters in healthy adults [13].

Apical long axis views	VARIABLES	MALE MEAN + SD	FEMALE MEAN + SD
GLS (%) (-19.10 ± 3.12)		-18.99 ± 3.08	-19.41 ± 3.27
2 CH View	GLS (%)	-20.83 ± 4.16	-20.72 ± 3.51
3 CH View	GLS (%)	-17.38 ± 3.17	-18.92 ± 3.42
4 CH View	GLS (%)	-19.12 ± 3.91	18.59 ± 4.97
Short axis views			
mv level	GCS (%)	-16.71 ± 6.55	-15.88 ± 6.01
	GRS (%)	23.11 ± 11.75	18.33 ± 6.70
pap muscle level	GCS (%)	-23.13 ± 6.52	-22.76 ± 7.06
	GRS (%)	25.10 ± 9.93	23.54 ± 11.07
GLS, global longitudinal strain; GCS, global circumferential strain; GRS, global radial strain; mv, mitral valve; pap, papillary; CH, chamber.			

CONCLUSION

Although MAD can be detected by TTE and TEE, it is only visualized during ventricular systole and may be missed and underreported especially in the absence of concomitant mitral valve disease. Recognition of MAD is particularly important given its association with life-threatening arrhythmic events and should especially be investigated in those with concomitant MVP or myxomatous MV disease with arrhythmias or symptoms of arrhythmias, therefore a multi-imaging modality approach may be necessary to improve detection. Imaging tools with

superior spatial resolution such as cardiac CT or CMR may serve as complementary diagnostic tools for those with a lesser degree of MAD. Detection of MAD by echocardiography is generally evaluated with a single plane image, which can overlook disjunction without the addition of three-dimensional imaging. CMR is considered the gold standard imaging technique for evaluating myocardial function, quantifying chambers and detecting scar. CMR has been shown to have more optimal detection of MAD compared to TTE and can provide risk stratification and prognostic information. Therefore CMR may be an important

adjunct to echocardiography as it can better define more subtle MAD and detect markers of arrhythmia risk.

2Dimensional STE with segmental longitudinal strain may allow for precise evaluation of the myocardium regarding subtle changes. According to the data from the literature, longitudinal strain could be a feasible indicator of future fibrosis appearance in LV segments and 2D STE strain analysis may allow for a more accurate assessment of the arrhythmic risk in MVP patients.

In our index patient, on performing 4D XStrain STE analysis there was a conspicuous reduction of magnitude of GLS and GCS values and furthermore the longitudinal segmental strain showed striking aberrations in multiple segments of LV. Perhaps, in future, this patient is a potential candidate for serious ventricular arrhythmias, even though he is presently asymptomatic.

Declaration by Authors

Acknowledgement: None

Source of Funding: None

Conflict of Interest: The authors declare no conflict of interest.

REFERENCES

1. Wunderlich NC, Ho SY, Flint N. Myxomatous mitral valve disease with mitral valve prolapse and mitral annular disjunction: clinical and functional significance of the coincidence. *J Cardiovasc Dev Dis.* 2021; 8:9
2. Faletra FF, Leo LA, Paiocchi VL, Pavan AG, Ho SY, Maisano F. Morphology of Mitral Annular Disjunction in Mitral Valve Prolapse. *Journal of the American Society of Echocardiography. JASE.* 2022; 35:176-186.
3. Bennett S, Thamman R, Griffiths T. Mitral annular disjunction: a systematic review of the literature. *Echocardiography.* 2019; 36:1549-1558
4. Essayagh B, Sabbag A, Antoine C. The mitral annular disjunction of mitral valve prolapse: presentation and outcome. *JACC Cardiovasc Imaging.* 2021; 14:2073-2087.
5. Garg P, Swift AJ, Zhong L, et al. Assessment of mitral valve regurgitation by cardiovascular magnetic resonance imaging. *Nat Rev Cardiol.* 2020; 17:298-312.
6. Zoghbi WA, Adams D, Bonow RO, et al. Recommendations for noninvasive evaluation of native valvular regurgitation: a report from the American Society of Echocardiography developed in collaboration with the Society for Cardiovascular Magnetic Resonance. *J Am Soc Echocardiogr.* 2017; 30:303-371.
7. Sheppard MN, Steriotis AK, Sharma S, Letter by Sheppard et al. Regarding Article, "Arrhythmic Mitral Valve Prolapse and Sudden Cardiac Death". *Circulation.* 2016;133: e458.
8. Alenazy A, Eltayeb A, Alotaibi MK, Anwar MK, Mulafikh N, Aladmawi M, Vriza O. Diagnosis of Mitral Valve Prolapse: Much More than Simple Prolapse. Multimodality Approach to Risk Stratification and Therapeutic Management. *J. Clin. Med.* 2022; 11:455.
9. Daniłowicz-Szymanowicz L, Zienciuk-Krajka A, Wabich E, Fijałkowski M, Fijałkowska J, Młodziński K and Raczak G. Left Ventricle Segmental Longitudinal Strain and Regional Myocardial Work Index Could Help Determine Mitral Valve Prolapse Patients with Increased Risk of Ventricular Arrhythmias. *J. Cardiovasc. Dev. Dis.,* 2023;10:181.
10. Huttin O, Pierre S, Venner C, Voilliot D, Sellal JM, Aliot E, Sadoul N, Juillièrè Y, Selton-Suty C. Interactions between mitral valve and left ventricle analysed by 2D speckle tracking in patients with mitral valve prolapse: one more piece to the puzzle, *European Heart Journal Cardiovascular Imaging,* 2017; 18:323-331.
11. Wang TKM, Kwon DH, Abou-Hassan O, Chetrit M, Harb SC, Patel D, Kalahasti V, Popovic ZB, Griffin BP, and Ayoub C. Strain evaluation for mitral annular disjunction by echocardiography and magnetic resonance imaging: A case-control study. *International journal of cardiology.* 2021; 33:154-156.
12. Muraru D, Cucchini U, Mihăilă S, Miglioranza MH, Aruta P, Cavalli G, Cecchetto A, Padayattil-Josè S, Peluso D, Illiceto S., Badano LP. Left Ventricular Myocardial Strain by Three-Dimensional Speckle-Tracking Echocardiography in

- Healthy Subjects: Reference Values and Analysis of Their Physiologic and Technical Determinants. *Journal of the American Society of Echocardiography*. 2014; 27:858-871.
13. Mehrotra A, Kacker S, Shadab M, Chandra N, Singh AK. 4 Dimensional XStrain speckle tracking echocardiography: comprehensive evaluation of left ventricular strain and twist parameters in healthy Indian adults during COVID-19 pandemic. *Am J Cardiovasc Dis*. 2022 15; 12:192-204.
 14. Sattur S, Bates S, Movahed MR. Prevalence of mitral valve prolapse and associated valvular regurgitations in healthy teenagers undergoing screening echocardiography *Exp Clin Cardiol*. 2010;15: e13-5.
 15. Cheng TO. Mitral valve prolapse: The Merchant of Venice or The Tales of Hoffman? *European Heart Journal*. 2002; 23:87-8.
 16. Watanabe C, Sugiura M, Ohkawa S, Ito Y, Toku A, Maeda S, et al Pathology and histochemistry of mitral valve prolapse *J Cardiol*. 1993; 23:69-77.
 17. Anders S, Said S, Schulz F, Püschel K. Mitral valve prolapse syndrome as cause of sudden death in young adults *Forensic Sci Int*. 2007;171:127-30.
 18. Edwards JESilver MD. Pathology of mitral incompetence *Cardiovascular Pathology*. New York, Edinburg Churchill Livingstone. 1983:575-98.
 19. Virmani R, Atkinson JB, Forman MB. The pathology of mitral valve prolapse *Herz*. 1988; 13:215-26.
 20. Bharati S, Granston A, Liebson P, Loeb H, Rosen K, Lev M. The Conduction System in Mitral Valve Prolapse Syndrome with Sudden Death. *Am Heart J*. 1981; 101:667-70.
 21. Hutchins G, Moore G, Skoog D. The Association of Floppy Mitral Valve with Disjunction of the Mitral Annulus Fibrosus. *N Engl J Med*. 1986; 314:535-40.
 22. Eriksson M, Bitkover C, Omran A et al. Mitral Annular Disjunction in Advanced Myxomatous Mitral Valve Disease: Echocardiographic Detection and Surgical Correction. *J Am Soc Echocardiogr*. 2005; 18:1014-22
 23. Konda T, Tani T, Furukawa Y. Mitral Annular Disjunction in Consecutive Cases: Echocardiographic Detection. *J Am Coll Cardiol*. 2013;61: E1046. 25.
 24. Konda T, Tani T, Suganuma N, Fujii Y, Ota M, Kitai T, Kaji S, Furukawa Y. Mitral annular disjunction in patients with primary severe mitral regurgitation and mitral valve prolapse. *Echocardiography*. 2020;37:1716-1722.
 25. Muthukumar L, Rahman F, Jan M et al. The Pickelhaube Sign: Novel Echocardiographic Risk Marker for Malignant Mitral Valve Prolapse Syndrome. *JACC Cardiovasc Imaging*. 2017; 10:1078-80.
 26. Drescher CS, Kelsey MD, Yankey GS, Sun AY, Wang A, Sadeghpour A, Glower DD, Vemulapalli S, Kelsey AM. Imaging Considerations and Clinical Implications of Mitral Annular Disjunction. *Journal*. 2022;15: e01423.
 27. Niarchou P, Prappa E, Liatakis I, Vlachos K, Chatziantoniou A, Nyktari E, Tse G, Efremidis M, Letsas KP. Mitral Valve Prolapse and Mitral Annular Disjunction Arrhythmic Syndromes: Diagnosis, Risk Stratification and Management. *Rev. Cardiovasc. Med*. 2022; 23:295.
 28. Toh H, Mori S, Izawa Y, Fujita H, Miwa K, Suzuki M, Takahashi Y, Toba T, Watanabe Y, Kono AK, et al. Prevalence and extent of mitral annular disjunction in structurally normal hearts: comprehensive 3D analysis using cardiac computed tomography. *Eur Heart J Cardiovasc Imaging*. 2021; 22:614-622.
 29. Mantegazza V, Volpato V, Gripari P, Ghulam Ali S, Fusini L, Italiano G, Murtatori M, Pontone G, Tamborini G, Pepi M. Multimodality imaging assessment of mitral annular disjunction in mitral valve prolapse. *Heart*. 2021; 107:25-32.
 30. Essayagh B, Iacuzio L, Civaia F, Avierinos JF, Tribouilloy C, Levy F. Usefulness of 3-tesla cardiac magnetic resonance to detect mitral annular disjunction in patients with mitral valve prolapse. *Am J Cardiol*. 2019; 124:1725-1730.
 31. Carmo P, Andrade MJ, Aguiar C, Rodrigues R, Gouveia R, Silva JA. Mitral annular disjunction in myxomatous mitral valve disease: a relevant abnormality recognizable by transthoracic echocardiography. *Cardiovasc Ultrasound*. 2010; 8:53.
 32. Perazzolo Marra M, Basso C, De Lazzari M, Rizzo S, Cipriani A, Giorgi B, Lacognata C, Rigato I, Migliore F, Pilichou K, et al. Morphofunctional abnormalities of mitral annulus and arrhythmic mitral valve

- prolapse. *Circ Cardiovasc Imaging*. 2016;9:e005030.
33. Lee AP, Jin CN, Fan Y, Wong RHL, Underwood MJ, Wan S. Functional implication of mitral annular disjunction in mitral valve prolapse: a quantitative dynamic 3D echocardiographic study. *JACC Cardiovasc Imaging*. 2017;10:1424-1433.
34. Özyıldırım S, Guven B, Yumuk MT, Barman HA, Dogan O, Topel C, Atici A, Donmez A, Kucukoglu MS, Dogan SM. Evaluation of left ventricular function in patients with mitral annular disjunction using speckle tracking echocardiography. *Echocardiography*. 2024 Apr;41(4):e15813. doi: 10.1111/echo.15813.

How to cite this article: Akhil Mehrotra, Faiz Illahi Siddiqui. Mitral annulus disjunction - an underdiagnosed anatomic morphology: review of literature. *International Journal of Science & Healthcare Research*. 2024; 9(4): 277-294. DOI: <https://doi.org/10.52403/ijshr.20240435>
